PERGAMON

Available online at www.sciencedirect.com

SCIENCE DIRECT®

International Journal of Non-Linear Mechanics 38 (2003) 1205–1219

INTERNATIONAL JOURNAL OF
NON-LINEAR
MECHANICS

www.elsevier.com/locate/ijnonlinmec

Large-scale statistical inverse computation of inelastic accretion in transient granular flows

T.I. Zohdi*

Department of Mechanical Engineering, 6195 Etcheverry Hall, University of California, Berkeley, CA 94720-1740, USA

Abstract

In this work, the accretion of fine-grained particulate matter into larger objects in high-speed granular flows, due to sudden disturbances in their mean velocity field, is investigated. A multibody collision model is developed whereby the coefficients of restitution and friction, as well as quantities such as the contact area and collision duration time, are implicit functions of the relative collision velocities and surfacial thermochemical reactions during impact. A recursive fixed-point multilayered staggering scheme is developed to simulate the resulting coupled non-linear system. Inverse problems are then constructed whereby transient flow conditions, reaction rates, particulate volume fractions, hardnesses, etc., are sought which deliver prespecified aggregate growth from a base starting particulate size. Classical gradient-based methods perform poorly, to this class of problems due to the fact that the associated objective functions depend in a non-convex and non-differentiable manner on the mentioned starting-state parameters. Furthermore, the results are very sensitive to the size of the control volumes selected. Therefore, due to the lack of robustness of classical gradient-based minimization schemes, a statistical genetic algorithm is developed whereby (I) the starting state-variables are represented by a "genetic string", and concepts of evolutionary behavior, such as selective reproduction, are applied to a population of such strings in order to determine an optimal set of starting state-parameters and (II) sequences of control volumes, each containing a finite number of particles, are adaptively computed until the sequential change in the ensemble average of a population of control volumes all fall below a given tolerance. Three-dimensional numerical examples are given to illustrate the behavior of the model and the overall solution process.

Keywords: Granular flows; Inelastic accretion; Inverse problems

1. Introduction

The study of granular media covers the behavior of materials such as sand, gravel, snow, interplanetary space dust, powders, sprays and pharmaceutical pills. The applications are broad. For example, over 50% (by weight) of the raw materials handled in chemical industries are granular media. Also, high-tech processes such as chemical vapor deposition, used in coating computer hardware, involve the analysis of particulate sprays. Another industrial application, concerned with granular flow, is the reduction of noise in aerodynamic designs [1]. Environmentally, the study of granular media is important for understanding the mechanics of landslides, coastal erosion and a host of other phenomena [2–5]. In particular, with regard to avalanche mechanics, we

* Tel.: +1-510-642-6834; fax: +1-510-642-6163.
E-mail address: zohdi@newton.berkeley.edu (T.I. Zohdi).

0020-7462/03/$ - see front matter © 2002 Published by Elsevier Science Ltd.
PII: S0020-7462(02)00066-5

refer the reader to the works of Hutter and collaborators: Tai et al. [6], Gray et al. [7], Wieland et al. [8], Berezin et al. [9], Gray and Hutter [10], Hutter [11], Hutter et al. [12], Hutter and Rajagopal [13], Koch et al. [14], Greve and Hutter [15] and Hutter et al. [16]. In another area, the space sciences, research is concerned with the formation of planetesimals by the aggregation of micron-sized granular dust particles in gaseous accretion disks [17–25]. The following general review articles, Jaeger and Nagel [26,27], Nagel [5], Jaeger and Nagel [28], Jaeger et al. [29–31], and Jaeger and Nagel [32], discuss the wide array of applications and research issues pertaining to granular media.

In many instances high-speed granular flows are encountered, where a primary concern is the accretion of the granular material into larger aggregates when such flows experience a sudden disturbance in their mean field. For example, industrially, this is important for quality control in vapor deposition processes, clogging of raw material feed lines, etc. Environmentally, for example in landslides, the concern is with the formation of large, potentially dangerous, aggregates. In the space sciences the concern is with the conditions required for planetesimals to form. In all of the mentioned cases, it is assumed, in one way or another, that grains collide, adhere, and grow into larger objects. For high-speed flow regimes, usually, for reasons of simplicity, at the simulation level, most studies simply arbitrarily assign a fixed low coefficient of restitution to the material surfaces, since otherwise the particles do not adhere [33]. However, it is well known that the coefficient of restitution is a function of the pressure that arises between the contacting surfaces. Other quantities, such as the friction forces, contact area and impact duration times, are also functions of the pressure, which implicitly depend on the relative velocity of the incoming and outgoing contact surfaces of the particles. For systems of particles, this leads to an enormous number of coupled non-linear equations. Historically, it is primarily for this reason that the implicit coupling has usually been ignored in simulations. However, the recent dramatic rise in computing power raises the possibility of more realistic modeling of the series of events leading to accretion, with the brunt of the effort shifted to numerical simulation.

The focus of the present work is on the modeling and simulation of inverse problems associated with the accretion of fine-grained particulates into larger objects collisions which involve possible thermo-chemical reactions at the contact surfaces. The outline of the presentation is as follows. In Section 2, a multibody collision model is developed whereby the coefficients of restitution and friction are functions of the impact velocities. In Section 3, other quantities such as the contact area and collision duration time, are expressed as implicit functions of the impact velocity. In Section 4, thermochemical reactions at the impact surfaces are modeled, and thermal softening, which affects accretion, is taken into account. In Section 5, a recursive fixed-point multilayered staggering scheme is developed to simulate the resulting coupled non-linear system. In Section 6, inverse problems are then constructed whereby transient flow conditions, reaction rates, particulate volume fractions, hardnesses, etc., are sought which deliver prespecified aggregate growth from a base starting particulate size. The results are very sensitive to the size of the control volumes selected. Furthermore, classical gradient-based methods perform poorly, or are simply inapplicable, due to the fact that the associated objective functions depend in a non-convex and non-differentiable manner on the mentioned starting-state parameters. Accordingly, a statistical genetic algorithm is developed whereby the starting-state variables are represented by a "genetic string", and evolutionary behavior, such as selective reproduction, is applied to a population of such strings to determine an optimal set of starting-state parameters and where sequences of control volumes, each containing a finite number of particles, are adaptively computed until the sequential change in the ensemble average of the population falls below a given tolerance. Finally, in Section 7, three-dimensional numerical examples are given to illustrate the behavior of the model and the overall solution process.

2. Momentum exchange, adhesion and friction

We consider a cloud of randomly distributed particles with random initial velocities. Two primary simplifying assumptions are made: (I) the particles, and any subsequent accretions that are formed, remain spherical,

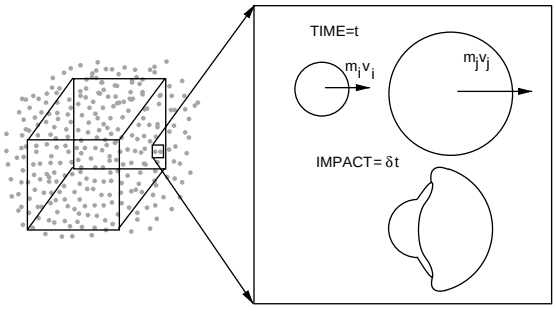

Fig. 1. The impact of two particles in a granular flow.

even after impact and (II) the accretions and particles do not (re)fissure upon impact. At time t, for two colliding particles i and j, normal to the line of impact, we have a conservation of momentum, before (t) and after $(t+\delta t)$ impact (Fig. 1),

$$m_i v_{in}^t + m_j v_{jn}^t = m_i v_{in}^{t+\delta t} + m_j v_{jn}^{t+\delta t}. \tag{1}$$

If one isolates one of the members of the colliding pair, then

$$m_i v_{in}^t + I_n \delta t = m_i v_{in}^{t+\delta t} \Rightarrow I_n = \frac{m_i (v_{in}^{t+\delta t} - v_{in}^t)}{\delta t}, \tag{2}$$

where I_n is the impulsive force between the particles. In addition to momentum transfer, an auxiliary relation comes from the commonly used material parameter, the coefficient of restitution, defined by the ratio of the relative velocities before and after impact

$$e \overset{\text{def}}{=} \frac{v_{jn}^{t+\delta t} - v_{in}^{t+\delta t}}{v_{in}^t - v_{jn}^t}. \tag{3}$$

If e were explicitly known, then one could write

$$v_{in}^{t+\delta t} = \frac{m_i v_{in}^t + m_j (v_{jn}^t - e(v_{in}^t - v_{jn}^t))}{m_i + m_j} \tag{4}$$

and

$$v_{jn}^{t+\delta t} = v_{in}^{t+\delta t} + e(v_{in}^t - v_{jn}^t). \tag{5}$$

However, the phenomenological material parameter (e) depends on I_n, and thus implicitly on the impact velocity. An approximate relation to determine whether two surfaces will bond when pressed together is if the magnitude of the surface pressure (P) exceeds or attains twice the Vicker's hardness $(2H)$, i.e. if $|P| \geqslant 2H$ then the particles will bond. See [34] for reviews. A typical value of the Vicker's hardness is $H \approx 3/\sigma_y$, where σ_y is the yield point for plastic deformation of the material. This is a relatively well-explored topic in the materials science literature. An obvious relation to approximate the surface pressure is $P \approx I_n/a^c$, where a^c represents the apparent contact area. Clearly if $e = 1$, the impact is purely elastic with no adhesion, and thus there is no loss in energy, while if $e = 0$ there is complete adhesion, and a maximum loss in energy. One can approximate e by a linear scaling with the pressure to hardness ratio

$$e \overset{\text{def}}{=} \frac{v_{jn}^{t+\delta t} - v_{in}^{t+\delta t}}{v_{in}^t - v_{jn}^t} \approx \max\left(1 - \frac{|I_n|/a^c}{2H}, 0\right) = \max\left(1 - \frac{m_i |v_{in}^{t+\delta t} - v_{in}^t|}{2a^c H \delta t}, 0\right). \tag{6}$$

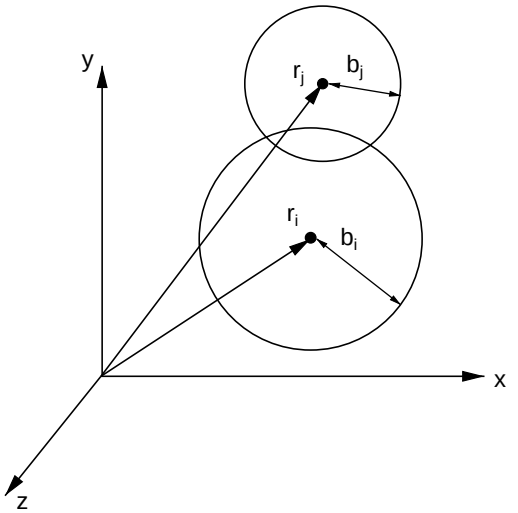

Fig. 2. Two contacting objects.

Since e is a function of the post-impact velocity, via $I_n = I_n(\boldsymbol{v}^{t+\delta t})$, Eqs. (4)–(6), along with relations that govern changes in other variables (contact area and friction) are strongly coupled. One approach, in fact the one adopted later in this work, to solve such a system is via a recursive (fixed-point type) staggering process, whereby one first assumes permanent adhesion $e = 0$, computing $v_{in}^{t+\delta t}$ and $v_{jn}^{t+\delta t}$, then one checks the implicit assumption of whether $|P| \geqslant 2H$ is correct. If $|P| < 2H$, then $e = 1 - |I_n|/2a^c H$ and the velocities are recomputed. The procedure is repeated until the difference between successive solutions is below a given tolerance. Essentially the same relations can be computed for all impacting pairs. This is elaborated upon further in the work.

For a general preimpact velocity field of a particle, the normal velocity is computed by taking the inner product $\boldsymbol{v} \cdot \boldsymbol{n}$, and projecting this in the normal direction. The normal direction, for two different sized particles contacting one another, is determined by the difference in the position vectors of their centers (Fig. 2), $\boldsymbol{n}^{ji} = (\boldsymbol{r}_j - \boldsymbol{r}_i)/\|\boldsymbol{r}_j - \boldsymbol{r}_i\|$. If the value of $\|\boldsymbol{r}_j - \boldsymbol{r}_j\|$ is smaller than the sum of the two radii, then contact occurs. The geometries of the particles and subsequent accretions are approximated as being spherical. The sizes of the accretions can be determined by their total mass, $\rho_i \frac{4}{3}\pi b_i^3 = nm_i \Rightarrow b_i = (nm_i/\rho_i \frac{4}{3}\pi)^{1/3}$, where n is the total number of particles in an accretion. At time t, the tangential velocities, which are orthogonal to the normal direction, are computed by the difference of $\boldsymbol{v}_{\mathrm{TAN}}^t = \boldsymbol{v}^t - \boldsymbol{v}_n^t$. Immediately after impact, the tangential velocities are computed by a conservation of momentum in the tangential plane. For the impacting pair as a whole, we have, in the tangential plane, $m_i \boldsymbol{v}_{\mathrm{TAN}i}^t + m_j \boldsymbol{v}_{\mathrm{TAN}j}^t = m_i \boldsymbol{v}_{\mathrm{TAN}i}^{t+\delta t} + m_j \boldsymbol{v}_{\mathrm{TAN}j}^{t+\delta t}$. If there is permanent adhesion, dictated by $P \geqslant 2H$, then $\boldsymbol{v}_{\mathrm{TAN}i}^{t+\delta t} = \boldsymbol{v}_{\mathrm{TAN}j}^{t+\delta t}$. If the particles do not permanently adhere, then a balance of momentum for each particle in the tangential directions dictates, under the assumption of Coulomb type friction, $\mu|I_n| =$ friction force opposite to the direction of relative motion,

$$v_{\mathrm{TAN}ix}^{t+\delta t} = \frac{\mu|I_n|\delta t}{m_i} \frac{v_{\mathrm{TAN}ix}^t - v_{\mathrm{TAN}jx}^t}{\|\boldsymbol{v}_{\mathrm{TAN}i}^t - \boldsymbol{v}_{\mathrm{TAN}j}^t\|} + v_{\mathrm{TAN}ix}^t,$$

$$v_{\mathrm{TAN}iy}^{t+\delta t} = \frac{\mu|I_n|\delta t}{m_i} \frac{v_{\mathrm{TAN}iy}^t - v_{\mathrm{TAN}jy}^t}{\|\boldsymbol{v}_{\mathrm{TAN}i}^t - \boldsymbol{v}_{\mathrm{TAN}j}^t\|} + v_{\mathrm{TAN}iy}^t,$$

$$
\begin{aligned}
v_{\mathrm{TAN}iz}^{t+\delta t} &= \frac{\mu |I_n| \delta t}{m_i} \frac{v_{\mathrm{TAN}iz}^t - v_{\mathrm{TAN}jz}^t}{\|\boldsymbol{v}_{\mathrm{TAN}i}^t - \boldsymbol{v}_{\mathrm{TAN}j}^t\|} + v_{\mathrm{TAN}iz}^t, \\
v_{\mathrm{TAN}jx}^{t+\delta t} &= \frac{\mu |I_n| \delta t}{m_j} \frac{v_{\mathrm{TAN}ix}^t - v_{\mathrm{TAN}jx}^t}{\|\boldsymbol{v}_{\mathrm{TAN}i}^t - \boldsymbol{v}_{\mathrm{TAN}j}^t\|} + v_{\mathrm{TAN}jx}^t, \\
v_{\mathrm{TAN}jy}^{t+\delta t} &= \frac{\mu |I_n| \delta t}{m_j} \frac{v_{\mathrm{TAN}iy}^t - v_{\mathrm{TAN}jy}^t}{\|\boldsymbol{v}_{\mathrm{TAN}i}^t - \boldsymbol{v}_{\mathrm{TAN}j}^t\|} + v_{\mathrm{TAN}jy}^t, \\
v_{\mathrm{TAN}jz}^{t+\delta t} &= \frac{\mu |I_n| \delta t}{m_j} \frac{v_{\mathrm{TAN}iz}^t - v_{\mathrm{TAN}jz}^t}{\|\boldsymbol{v}_{\mathrm{TAN}i}^t - \boldsymbol{v}_{\mathrm{TAN}j}^t\|} + v_{\mathrm{TAN}jz}^t.
\end{aligned} \tag{7}
$$

We take the friction coefficient to be a linear function of the coefficient of restitution $\mu = \mu_0(1-e)$. Therefore, in a consistent manner, if $e = 1$ it is an idealized, energy preserving, impact.

Remark. Immediately after impact, the particles must be slightly displaced in the direction of their outgoing velocities so that the particles no longer overlap. Algorithmically, the violation criterion is, $\theta \overset{\text{def}}{=} \|\boldsymbol{r}_i - \boldsymbol{r}_j\|/(b_i + b_j) < 1$, and the subsequent immediate post-impact updates are a function of the amount of particle overlap:

$$
\begin{aligned}
\boldsymbol{r}_i^{t+\delta t} &= \boldsymbol{r}_i^t + b_i^t(1-\theta^t)\frac{\boldsymbol{v}_i^{t+\delta t}}{\|\boldsymbol{v}_i^{t+\delta t}\|}, \\
\boldsymbol{r}_j^{t+\delta t} &= \boldsymbol{r}_j^t + b_j^t(1-\theta^t)\frac{\boldsymbol{v}_j^{t+\delta t}}{\|\boldsymbol{v}_j^{t+\delta t}\|}.
\end{aligned} \tag{8}
$$

To update the positions after the impact we use a Backward Euler approximation for all the particles in the system, where Δt is the discrete time step size:

$$
\begin{aligned}
r_{xi}^{t+\delta t+\Delta t} &= r_{xi}^{t+\delta t} + \Delta t v_{xi}^{t+\delta t}, \\
r_{yi}^{t+\delta t+\Delta t} &= r_{yi}^{t+\delta t} + \Delta t v_{yi}^{t+\delta t}, \\
r_{zi}^{t+\delta t+\Delta t} &= r_{zi}^{t+\delta t} + \Delta t v_{zi}^{t+\delta t}.
\end{aligned} \tag{9}
$$

Remark. Even though the particles may still slightly overlap after the application of the relations in Eq. (8), after the application of the relations in Eq. (9) they will be well separated.

3. Intrinsic time scales

One can directly obtain an estimate on the relative velocities needed for particle accretion by setting $e = 0$ in Eqs. (4)–(6). Assuming $m_i = m_j = m$ yields $v_{\mathrm{rel}}^{\mathrm{crit}} \overset{\text{def}}{=} v_{jn}^t - v_{in}^t = 4a^c H \delta t/m$. Since the particles are assumed to be spherical, the mass for each particle can be written as $m = \rho \frac{4}{3}\pi b^3$, where b is the radius. If we assume that the contact area is proportional to the cross-sectional area of the particles, $a^c = k\pi b^2$, $0 \leqslant k \leqslant 1$,

then

$$v_{\text{rel}}^{\text{crit}} = 3\frac{Hk\delta t}{b}. \tag{10}$$

In such a simple model, as b becomes larger, the critical velocity needed for adhesion becomes smaller, *provided that quantities like impact duration time and the contact area scaling are independent of particle size. However, this is unrealistic*. To correct this inadequacy, we assume that the contact area scales with the severity of impact, characterized by e. A relatively simple way to express this is by a linear function of the coefficient of restitution and cross-sectional area of the smaller of the two contacting bodies (Fig. 1),

$$a^c = (a_0 + (a_{\text{f}} - a_0)(1-e))\pi(\min(b_i, b_j))^2. \tag{11}$$

A logical relation for the impact duration time is the time to compress and decompress the radius of the smaller of the two impacting pairs,

$$\delta t = \frac{2\zeta \min(b_i, b_j)}{|v_{in}^t - v_{jn}^t| + |v_{in}^{t+\delta t} - v_{jn}^{t+\delta t}|} = \frac{2\zeta \min(b_i, b_j)}{(1+e)|v_{in}^t - v_{jn}^t|}, \tag{12}$$

where $0 < \zeta \leqslant 1$. Under these assumptions, to make an estimate of the critical velocities needed, we consistently modify Eq. (10) by assuming that the particles are of the same size, and that $e = 0$, thus leaving $v_{\text{rel}}^{\text{crit}} = \sqrt{6a_{\text{f}}H\zeta}$. We define the average separation distance (S) between particles as the control volume (V) divided by the number of particles (N), $L \overset{\text{def}}{=} (V/N)^{1/3}$, minus the diameter of an intrinsic particle (D), i.e. $S = L - D$. An estimate for the number of collision cycles (M) needed to drive the energy to steady state, i.e. to drive the relative velocities below a small tolerance, is given by $\bar{e}^M = \text{TOL} \Rightarrow M = \text{Ln}(\text{TOL})/\text{Ln}(\bar{e})$, where $\bar{e}$ is an estimate of the average coefficient of restitution in the system. To insure that the time duration of the simulation is long enough to reach steady state, a relatively conservative (high) value should be chosen for the average coefficient of restitution in the system, for example $\bar{e} \approx 0.9$, while a relatively low value should be chosen for the tolerance, for example $\text{TOL} = 0.01$. An approximate intrinsic simulation time scale (T) is the time it takes for one collision cycle, multiplied by the number of collision cycles to bring the system to steady state, therefore

$$T \approx \frac{S}{v_{\text{rel}}^{\text{crit}}} M. \tag{13}$$

Remark 1. Because the system will lose energy during the impact events, if the starting relative velocities are below the critical value, it is unlikely to have much significant accretion, since the system will progressively "lose its chances for accretion" due to energy losses.

Remark 2. For simulation purposes, we want no losses in energy and momentum in the system *due to particles escaping to the outside of each control volume*. Therefore, if a particle escapes from the control volume, it is placed on the opposite end of the control volume with the same (now incoming) velocity for the component direction violated, i.e. if $|r_x| \geqslant \text{limit}$, then $r_x = -\text{limit}\, r_x/|r_x|$. Therefore, the total system energy can decrease *only due to collision losses*. The momentum will remain constant, due to the fact that no external forces are applied.

4. Surfacial thermochemical effects

The strain rates in such impact scenarios can lead to locally high temperatures in the contact zone which, when coupled to thermochemical reactions, due to possibly reactive materials present on the surface of

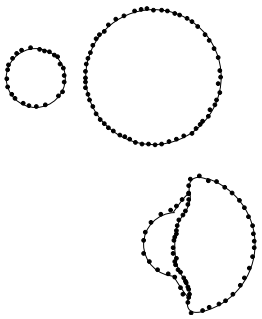

Fig. 3. A possible scenario where a film of hydrogen, or some other reactant, covers the surfaces of an impacting pair.

particles, may lead to a rapidly formed molten layer, which, upon cooling, strongly fuses the colliding pair together. In fact, this effect has been exploited in the materials processing community by purposely adding powdered hydrides and other potentially reactive materials into metallic powder mixes to enhance thermochemical bonding upon compaction. One such method is shock induced chemical reactions (SICR), whereby a shock wave is passed through chemical reacting powders, which sinters them together. Relevant work in the modeling and simulation of such processes can be found in [34–38] and recently in [39]. In another realm, planetesimal accretion, the presence of hydrogen gas adsorbed onto the surface of interplanetary debri is thought to be a possible explanation for easier bonding of particles upon impact (Fig. 3). Therefore, regardless of the specific application, it is reasonable to include such effects into the general model.

In order to incorporate thermochemical surface reaction effects that enhance accretion, we consider an energy balance for an impacting pair. We assume that all losses in kinetic energy are converted into heat, and that surface reactions in the contact zone provide additional energy. The post-collision velocities are computed from the momentum relations. The resulting kinetic energy loss is

$$W_{\mathrm{L}} \stackrel{\mathrm{def}}{=} \tfrac{1}{2}\, m_i \boldsymbol{v}_i^t \boldsymbol{v}_i^t + \tfrac{1}{2}\, m_j \boldsymbol{v}_j^t \boldsymbol{v}_j^t - \tfrac{1}{2} m_i \boldsymbol{v}_i^{t+\delta t} \boldsymbol{v}_i^{t+\delta t} - \tfrac{1}{2} m_j \boldsymbol{v}_j^{t+\delta t} \boldsymbol{v}_j^{t+\delta t}. \tag{14}$$

We assume that the forces of compression and restitution during an impact event are always equal and opposite between a colliding pair of particles in the contact zone, and also that the kinetic energy lost in the system is split equally between the impacting pair

$$m_i C \theta^{\,t+\delta t} = m_i C \theta^{\,t} + \frac{W_{\mathrm{L}}}{2} + \mathscr{R}_i, \tag{15}$$

where C is the heat capacity per unit mass, and $\mathscr{R}_i$ is the contribution from reactions at the surfaces of the particles. This term can be expressed as

$$\mathscr{R}_i = \alpha a^{\mathrm{c}} = \alpha(a_0 + (a_{\mathrm{f}} - a_0)(1-e))\pi(\min(b_i, b_j))^2, \tag{16}$$

where α is a material constant. For the particle pair, the new temperature can be written as

$$\theta_i^{t+\delta t} = \theta_i^t + \frac{W_{\mathrm{L}}}{2m_i C} + \frac{\alpha}{m_i C}\,(a_0 + (a_{\mathrm{f}} - a_0)(1-e))\pi(\min(b_i, b_j))^2,$$

$$\theta_j^{t+\delta t} = \theta_j^t + \frac{W_{\mathrm{L}}}{2m_j C} + \frac{\alpha}{m_j C}\,(a_0 + (a_{\mathrm{f}} - a_0)(1-e))\pi(\min(b_i, b_j))^2. \tag{17}$$

The temperature rise affects the impacting materials hardnesses, since $H \approx \sigma_y/3$, where σ_y is a function of temperature. Since the strain rates in such impact scenarios can lead to high particulate temperatures leading to thermal softening and potentially to melting, the threshold for strong bonding can be dramatically reduced. To model thermal softening, the hardness parameter H is represented by $H = H_0 e^{U/R\theta}$, where U is an activation energy and R is the universal gas constant, motivated by the fact that dislocation dynamics, the subcontinuum mechanism for continuum plastic flow, is usually governed by such an Arrhenius-type relation. *Clearly, these equations are coupled to those of impact*. After impact, it is assumed that the heat begins to be radiated away, governed by

$$\rho C \dot{\theta} = \nabla \cdot (\mathbb{K} \cdot \nabla \theta) + \mathscr{B}(\theta - \theta_0)^4, \tag{18}$$

where $\mathbb{K}$ is the material's conductivity, θ_0 is the ambient temperature, $\mathscr{B}$ is the Stefan–Boltzmann constant, $\mathscr{B} = -5.67 \times 10^{-8} \mathrm{N\,m/s\,K^{\circ}}$, and where, consistent with the particle-based philosophy, it is assumed that the temperature fields are uniform in the particles, thus $\nabla\theta = \mathbf{0}$. Therefore, after a single forward Euler integration, we have

$$\theta^{t+\delta t+\Delta t} = \theta^{t+\delta t} + \Delta t \left(\frac{\mathscr{B}}{\rho C} (\theta^{t+\delta t} - \theta_0)^4 \right). \tag{19}$$

Remark. Two central open issues are (1) the effect of particle and accretion topology, which clearly will not be spherical and (2) (re)fissuring of accretions and particles. To an extent, these issues can only be investigated further by more detailed analysis of the spatial deformation during impact within a large-scale multibody collision analyses. This is outside the scope of the present analysis. Possible extensions in this direction, amenable to large scale computation, may be to employ the concept of pseudo-rigid bodies. A pseudo-rigid body can only deform only homogeneously. For recent theoretical and numerical developments in this area we refer the reader to [40–42].

5. Multilayered fixed-point staggering schemes

We now address the solution of the system of equations generated by the model developed thus far. In order to do this, consider a general system of coupled non-linear equations given by $\mathscr{D}(\boldsymbol{z}) = \mathscr{F}$, where $\boldsymbol{z}$ is a solution, and where it is assumed that the operator, $\mathscr{D}$, is invertible. One desires that the sequence of iterated solutions, $\boldsymbol{z}^I$, $I = 1, 2, \ldots$, converges to $\mathscr{D}^{-1}(\mathscr{F})$ as $I \to \infty$. If $\boldsymbol{z}^I$ is a function of $\mathscr{D}, \mathscr{F}, \boldsymbol{z}^I, \ldots, \boldsymbol{z}^{I-K}$ one says that K is the order of iteration. It is assumed that the Ith iterate can be represented by $\boldsymbol{z}^I = \mathscr{G}^I(\boldsymbol{z}^{I-1}) + \boldsymbol{r}^I$. A necessary condition for convergence is iterative self consistency, i.e. $\mathscr{G}^I(\boldsymbol{z}) + \boldsymbol{r}^I = \boldsymbol{z}$, therefore $\boldsymbol{z} = \mathscr{D}^{-1}(\mathscr{F}) = \mathscr{G}^I(\mathscr{D}^{-1}(\mathscr{F})) + \boldsymbol{r}^I$. Accordingly, one has the consistency condition $\boldsymbol{r}^I = \mathscr{D}^{-1}(\mathscr{F}) - \mathscr{G}^I(\mathscr{D}^{-1}(\mathscr{F}))$, and as a consequence, $\boldsymbol{z}^I = \mathscr{G}^I(\boldsymbol{z}^{I-1}) + \mathscr{D}^{-1}(\mathscr{F}) - \mathscr{G}^I(\mathscr{D}^{-1}(\mathscr{F}))$. Using the consistency requirement, a sufficient condition for convergence can be obtained by defining the error vector: $\varepsilon^I = \boldsymbol{z}^I - \boldsymbol{z} = \boldsymbol{z}^I - \mathscr{D}^{-1}(\mathscr{F}) = \mathscr{G}^I(\boldsymbol{z}^{I-1}) + \mathscr{D}^{-1}(\mathscr{F}) - \mathscr{G}^I(\mathscr{D}^{-1}(\mathscr{F})) - \mathscr{D}^{-1}(\mathscr{F}) = \mathscr{G}^I(\boldsymbol{z}^{I-1}) - \mathscr{G}^I(\mathscr{D}^{-1}(\mathscr{F}))$. For the non-linear systems considered, a sufficient condition for convergence is the existence of a contraction mapping $\|\varepsilon^I\| = \|\boldsymbol{z}^I - \boldsymbol{z}\| = \|\mathscr{G}^I(\boldsymbol{z}^{I-1}) - \mathscr{G}^I(\boldsymbol{z})\| \leqslant |\mathscr{K}|\,\|\boldsymbol{z}^{I-1} - \boldsymbol{z}\|$, where if $|\mathscr{K}| < 1$ for each iteration I, then $\varepsilon^I \to \mathbf{0}$ for any arbitrary starting solution $\boldsymbol{z}^{I=0}$ as $I \to \infty$. See [43] or [44] for reviews. A multilevel (embedded) recursive

staggering implementation of such a scheme, applied to the problem of interest, is as follows:

(1) FOR EACH PARTICLE (i) FIND CURRENT NEAREST NEIGHBOR (j) : $r_j \stackrel{\text{def}}{=} \min_{r_p, p\neq i} \|\boldsymbol{r}_i - \boldsymbol{r}_p\|$
(2) IF CONTACT CRITERIA MET ASSUME COMPLETE ADHESION ($K=0,\ e^K=0$) :
(3) COMPUTE THE FOLLOWING FOR THE CONTACT PAIR :

$$v_{in}^{t+(\delta t)^K} = \frac{m_i v_i^t + m_j (v_j^t - e^K (v_{in}^t - v_{jn}^t))}{m_i + m_j}$$

$$v_{jn}^{t+(\delta t)^K} = v_{in}^{t+(\delta t)^K} + e^K (v_{in}^t - v_{jn}^t)$$

$$I_n^K = \frac{m_i (v_{in}^{t+(\delta t)^K} - v_{in}^t)}{(\delta t)^K}$$

$$v_{\mathrm{TAN}ix}^{t+(\delta t)^K} = -\frac{\mu |I_n^K| (\delta t)^K}{m_i} \frac{v_{\mathrm{TAN}ix}^t - v_{\mathrm{TAN}jx}^t}{\|\boldsymbol{v}_{\mathrm{TAN}i}^t - \boldsymbol{v}_{\mathrm{TAN}j}^t\|} + v_{\mathrm{TAN}ix}^t,$$

$$v_{\mathrm{TAN}iy}^{t+(\delta t)^K} = -\frac{\mu |I_n^K| (\delta t)^K}{m_i} \frac{v_{\mathrm{TAN}iy}^t - v_{\mathrm{TAN}jy}^t}{\|\boldsymbol{v}_{\mathrm{TAN}i}^t - \boldsymbol{v}_{\mathrm{TAN}j}^t\|} + v_{\mathrm{TAN}iy}^t,$$

$$v_{\mathrm{TAN}iz}^{t+(\delta t)^K} = -\frac{\mu |I_n^K| (\delta t)^K}{m_i} \frac{v_{\mathrm{TAN}iz}^t - v_{\mathrm{TAN}jz}^t}{\|\boldsymbol{v}_{\mathrm{TAN}i}^t - \boldsymbol{v}_{\mathrm{TAN}j}^t\|} + v_{\mathrm{TAN}iz}^t,$$

$$v_{\mathrm{TAN}jx}^{t+(\delta t)^K} = \frac{\mu |I_n^K| (\delta t)^K}{m_j} \frac{v_{\mathrm{TAN}ix}^t - v_{\mathrm{TAN}jx}^t}{\|\boldsymbol{v}_{\mathrm{TAN}i}^t - \boldsymbol{v}_{\mathrm{TAN}j}^t\|} + v_{\mathrm{TAN}jx}^t,$$

$$v_{\mathrm{TAN}jy}^{t+(\delta t)^K} = \frac{\mu |I_n^K| (\delta t)^K}{m_j} \frac{v_{\mathrm{TAN}iy}^t - v_{\mathrm{TAN}jy}^t}{\|\boldsymbol{v}_{\mathrm{TAN}i}^t - \boldsymbol{v}_{\mathrm{TAN}j}^t\|} + v_{\mathrm{TAN}jy}^t,$$

$$v_{\mathrm{TAN}jz}^{t+(\delta t)^K} = \frac{\mu |I_n^K| (\delta t)^K}{m_j} \frac{v_{\mathrm{TAN}iz}^t - v_{\mathrm{TAN}jz}^t}{\|\boldsymbol{v}_{\mathrm{TAN}i}^t - \boldsymbol{v}_{\mathrm{TAN}j}^t\|} + v_{\mathrm{TAN}jz}^t.$$

IF $\dfrac{|I_n^K|}{a^K} \geqslant 2H$ THEN ACCRETE m_i AND m_j INTO ONE PARTICLE $= m_i + m_j$

$$e^{K+1} \stackrel{\text{def}}{=} \max\left(1 - \frac{m_i |v_{in}^{t+(\delta t)^K} - v_{in}^t|}{a^{\mathrm{c},K} 2H (\delta t)^K}, 0\right)$$

IF $|e^{K+1} - e^K| \leqslant e^K \mathrm{TOL}$ THEN GO TO (2) FOR NEXT CONTACT PAIR

IF $|e^{K+1} - e^K| > e^K \mathrm{TOL}$ THEN

$$e^K = e^{K+1}$$

$$(\delta t)^{K+1} = \frac{2k \min(b_i, b_j)}{(|v_{in}^t - v_{jn}^t| + |v_{in}^{t+(\delta t)^K} - v_{jn}^{t+(\delta t)^K}|)},$$

$$a^{c,K+1} = (a_0 + (a_\mathrm{f} - a_0)(1 - e^{K+1}))\pi(\min(b_i, b_j))^2.$$

$$W_L^{K+1} \stackrel{\text{def}}{=} \frac{1}{2}\left(m_i \boldsymbol{v}_i^t \cdot \boldsymbol{v}_i^t + m_j \boldsymbol{v}_j^t \cdot \boldsymbol{v}_j^t - m_i \boldsymbol{v}_i^{t+(\delta t)^{K+1}} \cdot \boldsymbol{v}_i^{t+(\delta t)^{K+1}} - m_j \boldsymbol{v}_j^{t+(\delta t)^{K+1}} \cdot \boldsymbol{v}_j^{t+(\delta t)^{K+1}}\right),$$

$$\theta_i^{t+(\delta t)^{K+1}} = \theta_i^t + \frac{W_L^{K+1}}{2 m_i C} + \frac{\alpha}{m_i C}(a_0 + (a_\mathrm{f} - a_0)(1 - e^{K+1}))\pi(\min(b_i, b_j))^2,$$

$$\theta_j^{t+(\delta t)^{K+1}} = \theta_j^t + \frac{W_L^{K+1}}{2 m_j C} + \frac{\alpha}{m_j C}(a_0 + (a_\mathrm{f} - a_0)(1 - e^{K+1}))\pi(\min(b_i, b_j))^2,$$

GO TO (2) AND REPEAT FOR THE NEXT CONTACT PAIR
(4) UPDATE VELOCITIES, POSITIONS, TEMPERATURES ETC … AND GO TO (1) (20)

Remark. Typically, for the system at hand, convergence is easily attained over a wide parameter range, since at low speeds the contraction constant is small, and the iterations converge quickly, while at high speeds, the particles accrete ($e = 0$), and only a few iterations are necessary.

6. Statistical inverse solution schemes

We now concentrate on constructing inverse problems where transient flow conditions, reaction rates, particulate volume fractions, hardnesses, etc., are sought which deliver prespecified aggregate growth from a base starting particulate size. For example consider the cost function, $\Pi = |(1/2)(b^{\mathrm{f}}/b^0) - 1|$, where b^{f} is the final average radius of the particles in a control volume and b^0 is average radius at the starting state. Due to the fact that objective functions such as Π depend in a non-convex and non-differentiable manner on the mentioned starting-state parameters, gradient-based minimization methods are inapplicable. The lack of *robustness* of gradient-based deterministic minimization processes can be rectified by application of a family of methods, usually termed "genetic" algorithms. Genetic algorithms are search methods based on the principles of natural selection, employing concepts of species evolution, such as reproduction, mutation and crossover. Such methods stem from the work of John Holland and his colleagues in the late 1960s and early 1970s at the University of Michigan [45]. For reviews of such methods, the interested reader is referred to Goldberg [46], Davis [47] and Onwubiko [48]. A recent overview of the state of the art of the field can be found in a collection of recent articles, edited by Goldberg and Deb [49].

In [50] a genetic algorithm was developed, where the key feature was the development of a "genetic string", which contains microstructural design information. A "survival of the fittest" algorithm was then applied to a population of such strings. In this presentation, we concentrate on adapting this type of genetic algorithm to inverse problems. Accordingly, we write the state vector as a string

$$\boldsymbol{\Lambda} \stackrel{\mathrm{def}}{=} (\boldsymbol{v}^0_{\mathrm{rel}}, s, \rho, H_0, C, \mu_0, \theta_0, U, \alpha) \tag{21}$$

and apply the following:

Step 1: RANDOMLY SELECT N STARTING GENETIC STRINGS $\boldsymbol{\Lambda}^i \stackrel{\mathrm{def}}{=} \{\Lambda^i_1, \Lambda^i_2, \ldots,\}$ $(i = 1, \ldots, N)$:

Step 2: COMPUTE FITNESS $(\Pi(\boldsymbol{\Lambda}^i))$ OF EACH GENETIC STRING : $(i = 1, \ldots, N)$

Step 3: RANK THE GENETIC STRINGS, $\boldsymbol{\Lambda}^i$ $(i = 1, \ldots, N)$

Step 4: MATE NEAREST PAIRS (PRODUCE OFFSPRING) $(i = 1, \ldots, N)$

$$\boldsymbol{\lambda}^i \stackrel{\mathrm{def}}{=} \boldsymbol{\Phi}^i \boldsymbol{\Lambda}^i + (1 - \boldsymbol{\Phi}^i)\boldsymbol{\Lambda}^{i+1} \quad \boldsymbol{\lambda}^{i+1} \stackrel{\mathrm{def}}{=} \boldsymbol{\Phi}^{i+1} \boldsymbol{\Lambda}^{i+1} + (1 - \boldsymbol{\Phi}^{i+1})\boldsymbol{\Lambda}^{i+1}$$

$$0 \leqslant \boldsymbol{\Phi}^i = \mathbf{RAND} \leqslant 1 \ (\textit{DIFFERENT FOR EACH COMPONENT})$$

Step 5: ENFORCE CONSTRAINTS : $\boldsymbol{\Lambda}^{i-} \leqslant \boldsymbol{\Lambda}^i \leqslant \boldsymbol{\Lambda}^{i+}$

Step 6: KILL OFF BOTTOM $M < N$ STRINGS. OPTIONAL : KEEP TOP K PARENTS

Step **7:** REPEAT WITH TOP GENE POOL PLUS $\boldsymbol{M}$ NEW ONES : $\boldsymbol{\Lambda^i = \Lambda^i}$, $\boldsymbol{(i = 1, \ldots, N)}$

Termination : REPEAT UNTIL $\|\Pi\| \leqslant$ TOL (22)

We remark that the definition of "fitness" of a genetic string in this algorithm indicates the value of the objective function. In other words, the most fit genetic string is simply the one with the smallest objective

function.[1] At first glance, it may seem inconsequential to retain the top parents, however, in [50], it was found that parent retention produces superior results. This stems from the fact that the objective functions are highly non-convex, consequently there exists a strong possibility that inferior offspring will replace superior parents. Therefore, the practice of retaining the top parents is not only less computationally expensive, since they do not have to be reevaluated, it is theoretically superior. With top parent retention, the minimization of the cost function is guaranteed to be monotone. The total number of global evaluations is equal to $q+(g-1)\times(q-p)$, where g is the number of generations, q is the total number of genetic strings in the population, and p if the number of parents kept after each generation.

6.1. Stabilization of statistically uncertain systems

An idealized steady-state system energy can be computed from the fact that each individual particle's velocity can be split into the mean and perturbed part, $\boldsymbol{v}_i = \langle \boldsymbol{v}_i \rangle + \delta \boldsymbol{v}_i$, where $\langle \delta \boldsymbol{v}_i \rangle = \boldsymbol{0}$

$$\begin{aligned}
\text{Kinetic energy} &= \frac{1}{2}\sum_{i=1}^{N} m_i(\langle \boldsymbol{v}_i \rangle + \delta \boldsymbol{v}_i)\cdot(\langle \boldsymbol{v}_i \rangle + \delta \boldsymbol{v}_i) \\
&= \frac{1}{2}\sum_{i=1}^{N} m_i \langle \boldsymbol{v}_i \rangle \cdot \langle \boldsymbol{v}_i \rangle + \sum_{i=1}^{N} m_i \langle \boldsymbol{v}_i \rangle \cdot \delta \boldsymbol{v}_i + \frac{1}{2}\sum_{i=1}^{N} m_i \delta \boldsymbol{v}_i \cdot \delta \boldsymbol{v}_i \\
&= \frac{1}{2}\sum_{i=1}^{N} m_i \langle \boldsymbol{v}_i \rangle \cdot \langle \boldsymbol{v}_i \rangle + \frac{1}{2}\sum_{i=1}^{N} m_i \delta \boldsymbol{v}_i \cdot \delta \boldsymbol{v}_i. \qquad (23)
\end{aligned}$$

If there is no energy input into the system, as the inelastic collisions progress ($e < 1$), then the system kinetic energy will tend towards $\frac{1}{2}\sum_{i=1}^{N} m_i \langle \boldsymbol{v}_i \rangle \cdot \langle \boldsymbol{v}_i \rangle$ since $e(v_{in}^t - v_{jn}^t) = v_{jn}^{t+\delta t} - v_{in}^{t+\delta t} \to 0$ as $t \to \infty$. Typically, for particle groups with a finite number of grains, for example several hundred, a numerically generated (random) sample realization will not be perfectly statistically representative, i.e. $\langle \delta \boldsymbol{v}_i \rangle \neq \boldsymbol{0}$. Therefore, one must simulate several samples and then ensemble average the responses of the samples to obtain statistically valid objective functions.

6.2. Convergence in the sense of statistical moments

The exact number of tests needed to stabilize the results is controlled by the characteristics of the statistical distribution of responses associated with a starting-state vector. One can describe the essential characteristics of distributions through statistical moments. Consider any tested quantity, Q, with a distribution of values ($Q_i,\ i = 1,2,\ldots,N = \text{samples}$) about an arbitrary reference point, denoted $Q^{\star}$, as follows:

$$\boldsymbol{M}_r^{Q_i - Q^{\star}} \overset{\text{def}}{=} \frac{\sum_{i=1}^{N}(Q_i - Q^{\star})^r}{N} \overset{\text{def}}{=} \overline{(Q_i - Q^{\star})^r}, \qquad (24)$$

where $\sum_{i=1}^{N}(\cdot)/N \overset{\text{def}}{=} \overline{(\cdot)}$ and $A \overset{\text{def}}{=} \overline{Q_i}$. The various moments characterize the distribution, for example: (I) $\boldsymbol{M}_1^{Q_i - A}$ measures the first deviation from the average, which equals zero, (II) $\boldsymbol{M}_1^{Q_i - 0}$ is the average, (III) $\boldsymbol{M}_2^{Q_i - A}$ is the standard deviation, (IV) $\boldsymbol{M}_3^{Q_i - A}$ is the skewness and (V) $\boldsymbol{M}_4^{Q_i - A}$ is the kurtosis. The higher moments, such as the skewness measure the bias, or asymmetry of the distribution of data, while the kurtosis measures

[1] It is remarked that if the function Φ is allowed to be greater than unity, one can consider the resulting convex combination (offspring) as a "mutation". Mutation was not used in the present work.

the degree of peakedness of the distribution of data around the average. The skewness is zero for symmetric data. A general criterion for ensemble convergence essentially suggests itself, namely, one should successively test samples with different random realizations until the relative difference between ensemble averages of the moments stabilize ($r = 1, 2, 3, \ldots$).

$$|\boldsymbol{M}_r^{Q_i^K - A^K} - \boldsymbol{M}_r^{Q_i^{K+1} - A^{K+1}}| \leqslant \mathrm{TOL}\,|\boldsymbol{M}_r^{Q_i^{K+1} - A^{K+1}}|, \tag{25}$$

where Q_i^K are the particles that have been computed from *all tests up to and including test K* and where A^K is the corresponding average.

7. Numerical experiments

We considered control volumes, each containing 100 initially non-intersecting particles. A population of 20 genetic strings was selected per generation. The top six parents were retained after each generational "mating sequence". The top six offspring were produced, and allowed to proceed, along with the top six parents, to the next generation. Therefore, eight old "bad" genetic strings were eliminated and eight new genetic strings were infused after each generation. For each starting state, 200 time steps were taken over the corresponding characteristic time scale (T) to insure adequate numerical accuracy.[2] The following impact parameters were chosen: $a_0 = 0.01$, $a_f = 1$ and $\zeta = 0.000001$. The initial position vectors were given random values, within each control volume of $-\mathscr{L} \leqslant r_{ix}, r_{iy}, r_{iz} \leqslant \mathscr{L}$. We considered starting-state vectors, constrained within prespecified search ranges, consisting of the relative velocity vector distribution $\boldsymbol{v}_{\mathrm{rel}} = \boldsymbol{v}_{\mathrm{rel}}^0 r_i$, where $0 \leqslant r_i \leqslant 1$, for each ($i$) particle, the diameter of the particles, which is scaled as follows, $s = d/(V/N)^{1/3}$, where $s^- \leqslant s \leqslant s^+$, the density of the particles $\rho^- \leqslant \rho \leqslant \rho^+$, the base hardness of the particles $H_0^- \leqslant H_0 \leqslant H_0^+$, the heat capacity of the particles $C^- \leqslant C \leqslant C^+$, the base coefficient of friction of the particles $\mu_0^- \leqslant \mu_0 \leqslant \mu_0^+$, the activation energy $U^- \leqslant U \leqslant U^+$ and the chemical reaction coefficient $\alpha^- \leqslant \alpha \leqslant \alpha^+$. The objective was to double the average particulate size at steady state ($t = T$) of the top six genetic strings

$$\Pi = \frac{1}{6}\sum_{k=1}^{6}\left|\frac{1}{2}\frac{b_k^{\mathrm{f}}}{b_k^0} - 1\right|, \tag{26}$$

where b_k^{f} is the final average radius of the particles for string k, i.e. the first moment of the particulate population distribution, at steady state, and b_k^0 is average radius at the starting state. The tolerance for convergence of the first moment of the distribution of radii (the average) was set to 0.00001,

$$|(b_k^{\mathrm{f}})^{J+1} - (b_k^{\mathrm{f}})^J| \leqslant \mathrm{TOL}|(b_k^{\mathrm{f}})^{J+1}|, \tag{27}$$

where $b_k^{\mathrm{f}} = \sum_{i=1}^{J} b_k^{\mathrm{f}i}/J$ and where J is the number of samples. The ranges of search for the state vector were

$$0.1\ \mathrm{m/s} \leqslant \boldsymbol{v}_{x\mathrm{rel}}^0 \leqslant 30\ \mathrm{m/s},$$

$$0.4 \leqslant s \leqslant 0.8,$$

$$10^3\ \mathrm{kg/m^3} \leqslant \rho \leqslant 10^4\ \mathrm{kg/m^3},$$

$$10\ \mathrm{MPa} \leqslant H_0 \leqslant 200\ \mathrm{MPa},$$

$$10\ \mathrm{J/Kg\text{-}(K^\circ)} \leqslant C \leqslant 1.5 \times 10^3\ \mathrm{J/Kg\text{-}(K^\circ)},$$

[2] The results were insensitive to refinement of discretization.

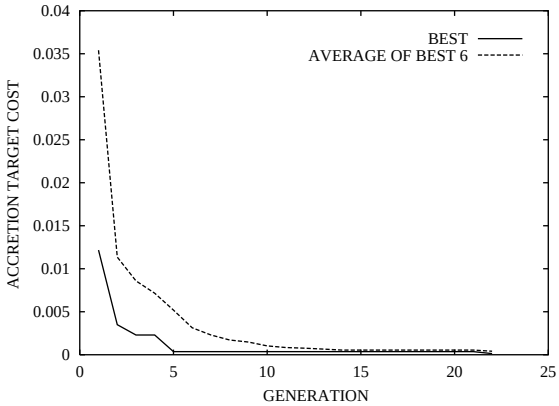

Fig. 4. Cost of best starting-state vectors and average of the top six after 22 generations.

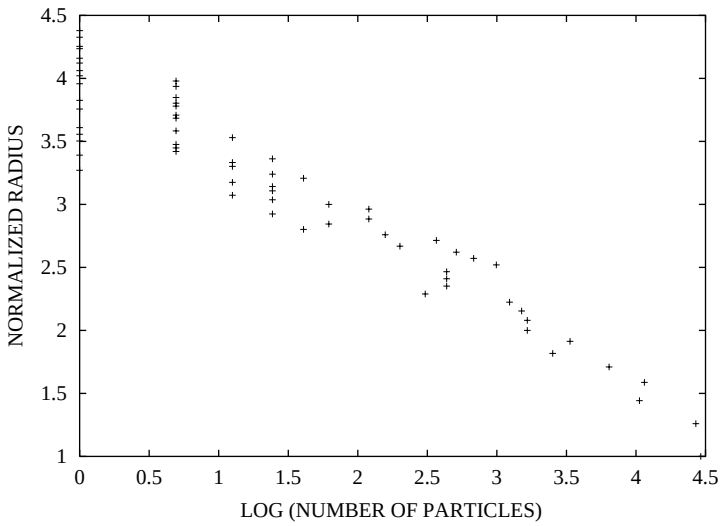

Fig. 5. For the best starting-state vector, the distribution of the normalized radii, defined as the final radii divided by the initial radius, for 89 control volumes (the number needed for statistical moment convergence, TOL $= 10^{-5}$), each with 100 particles. The simulation was driven to steady state ($T =$ the characteristic time scales).

$$
\begin{aligned}
&10^{-2} \leqslant \mu_0 \leqslant 0.5,\\
&273.13\ \mathrm{K}^\circ \leqslant \theta_0 \leqslant 373.13\ \mathrm{K}^\circ,\\
&10\ \mathrm{kJ/mol} \leqslant U \leqslant 10^3\ \mathrm{kJ/mol},\\
&0\ \mathrm{J/m^2} \leqslant \alpha \leqslant 10^7\ \mathrm{J/m^2},
\end{aligned}
\tag{28}
$$

where $v^0_{y\mathrm{rel}} = v^0_{z\mathrm{rel}} = 0$, i.e. a velocity field with only a non-zero *mean x* velocity component. Twenty-two generations were needed to meet an average tolerance of $\Pi \leqslant 0.0005$ *for the top six genetic strings*. A total of 314 genetic strings were tested. An average of 125 samples were needed per genetic string for a total of 39,286 samples tested (see Figs. 4 and 5, Table 1).

Table 1
Best starting-state vectors after 22 generations

Rank	v^0_{xrel} (m/s)	s	ρ (kg/m^3)	H_0 (MPa)	C (J/Kg-K$^\circ$)	μ_0	θ_0 (K$^\circ$)	U (kJ/mol)	α (J/m^2)	Π
1	4.326	0.633	6141.898	67.188	1279.542	0.307	330.652	707.351	5,940,883.989	0.00013602
2	4.746	0.638	5579.604	60.730	1170.780	0.283	353.865	598.416	2,347,406.359	0.00036241
3	4.434	0.637	5921.768	62.759	1310.642	0.292	349.057	578.921	3,157,762.434	0.00036671
4	3.412	0.621	6436.049	76.611	1339.450	0.308	327.914	573.144	3,864,868.553	0.00039773
5	3.074	0.626	5292.318	60.678	1114.462	0.311	335.793	751.632	6,910,186.063	0.00050522
6	4.257	0.632	6124.641	62.269	1265.586	0.308	335.316	709.750	6,790,030.553	0.00070812

In the previous example, the objective function centered on obtaining an average accretion size in the flow. Clearly, higher moments of the particle distributions can also be targeted. In this regard, convenient dimensionless higher-order moment measures of the particulate distribution can be represented through

$$m_r^{Q_i-A} = \frac{\boldsymbol{M}_r^{Q_i-A}}{\left(\sqrt{\boldsymbol{M}_2^{Q_i-A}}\right)^r}, \tag{29}$$

where (I) $m_1^{Q_i-A} = 0$, (II) $m_2^{Q_i-A} = 1$, (III) $m_3^{Q_i-A} = 0$ for symmetric data (IV) $m_4^{Q_i-A} = 3$ for a "normal" Gaussian distribution (V) $m_4^{Q_i-A} > 3$ for more peaked than Gaussian distribution (Leptokurtic) and (VI) $m_4^{Q_i-A} < 3$ for flatter than Gaussian distribution (Platykurtic). The fourth normalized moment is particularly useful to characterize the "peakedness" of the distribution. Such "higher moment" inverse problems studies are currently under investigation by the author.

Acknowledgements

The author expresses his gratitude to Prof. Philip Marcus for discussions on planetesimal accretion research currently underway in the astrophysics community.

References

[1] C.-h. Liu, S.R. Nagel, Sound in a granular material: disorder and nonlinearity, Phys. Rev. B 48 (1993) 15646.
[2] S.N. Coppersmith, C.-h. Liu, S. Majumdar, O. Narayan, T.A. Witten, Model of force fluctuations in bead packs, Phys. Rev. E 53 (1996) 4673.
[3] L.P. Kadanoff, S.R. Nagel, L. Wu, S.-m. Zhou, Scaling and universality in avalanches, Phys. Rev. A 39 (1989) 6527.
[4] C.-h. Liu, H.M. Jaeger, S.R. Nagel, Finite size effects in a sandpile, Phys. Rev. A 43 (1991) 7091.
[5] S.R. Nagel, Instabilities in a Sandpile, Rev. Mod. Phys. 64 (1992) 321.
[6] Y.-C. Tai, J.M.N.T. Gray, K. Hutter, S. Noelle, Flow of dense avalanches past obstructions, Ann. Glaciol. 32 (2001) 281–284.
[7] J.M.N.T. Gray, M. Wieland, K. Hutter, Gravity-driven free surface flow of granular avalanches over complex basal topography, Proc. Roy. Soc. London A 455 (1999) 1841–1874.
[8] M. Wieland, J.M.N.T. Gray, K. Hutter, Channelized free-surface flow of cohesionless granular avalanches in a chute with shallow lateral curvature, J. Fluid Mech. 1999 (392) 73–100.
[9] Y.A. Berezin, K. Hutter, L.A. Spodareva, Stability properties of shallow granular flows, Int. J. Non-Linear Mech. 33 (4) (1998) 647–658.
[10] J.M.N.T. Gray, K. Hutter, Pattern formation in granular avalanches, Cont. Mech. Thermodyn. 9 (1997) 341–345.
[11] K. Hutter, Avalanche dynamics, in: V.P. Singh (Ed.), Hydrology of Disasters, Kluwer Academic Publishers, Dordrecht, 1996, pp. 317–394.

[12] K. Hutter, T. Koch, C. Plss, S.B. Savage, The dynamics of avalanches of granular materials from initiation to runout. Part II. Experiments, Acta Mech. 109 (1995) 127–165.
[13] K. Hutter, K.R. Rajagopal, On flows of granular materials, Cont. Mech. Thermodyn. 6 (1994) 81–139.
[14] T. Koch, R. Greve, K. Hutter, Unconfined flow of granular avalanches along a partly curved surface. II. Experiments and numerical computations, Proc. Roy. Soc. London A 445 (1994) 415–435.
[15] R. Greve, K. Hutter, Motion of a granular avalanche in a convex and concave curved chute: experiments and theoretical predictions, Philos. Trans. Roy. Soc. London, A 342 (1993) 573–600.
[16] K. Hutter, M. Siegel, S.B. Savage, Y. Nohguchi, Two-dimensional spreading of a granular avalanche down an inclined plane. Part I: Theory, Acta Mech. 100 (1993) 37–68.
[17] J. Barranco, P. Marcus, O. Umurhan, Scaling and asymptotics of coherent vortices in protoplanetary disks, in: Studying Turbulence Using Numerical Simulation. Databases-VIII, Center for Turbulence Research, Proceedings of the Summer Program, Stanford University Press, Stanford, CA, 2001.
[18] J. Barranco, P. Marcus, Vortices in protoplanetary disks and the formation of planetesimals, in: Studying Turbulence Using Numerical Simulation. Databases-VIII, Center for Turbulence Research, Proceedings of the Summer Program, Stanford University Press, Stanford, CA, 2001.
[19] K.R. Grazier, W.I. Newman, W.M. Kaula, J.M. Hyman, Dynamical evolution of planetesimals in the outer solar system I. The Jupiter/Saturn zone, Icarus 140 (2) (1999) 341–352.
[20] K.R. Grazier, W.I. Newman, F. Varadi, W.M. Kaula, J.M. Hyman, Dynamical evolution of planetesimals in the outer solar system II. The Saturn/Uranus and Uranus/Neptune zones, Icarus 140 (2) (1999) 353–368.
[21] E. Kokubo, S. Ida, Formation of protoplanets from planetesimals in the solar nebula, Icarus 143 (1) (2000) 15–270.
[22] E. Kokubo, S. Ida, On runaway growth of planetesimals, Icarus 123 (1) (1996) 180–191.
[23] K.D. Supulver, D.N.C. Lin, Formation of icy planetesimals in a turbulent solar nebula, Icarus 146 (2) (2000) 525–540.
[24] P. Tanga, A. Babiano, B. Dubrulle, A. Provenzale, Forming planetesimals in vortices, Icarus 121 (1) (1996) 158–170.
[25] S.J. Weidenschilling, D. Spaute, D.R. Davis, F. Marzari, K. Ohtsuki, Accretional evolution of a planetesimal swarm, Icarus 128 (2) (1997) 429–455.
[26] H.M. Jaeger, S.R. Nagel, La Physique de l'Etat Granulaire, La Recherche 249 (1992) 1380.
[27] H.M. Jaeger, S.R. Nagel, Physics of the granular state, Science 255 (1992) 1523.
[28] H.M. Jaeger, S.R. Nagel, La Fisica del Estado Granular, Mundo Cientifico 132 (1993) 108.
[29] H.M. Jaeger, J.B. Knight, C.-h. Liu, S.R. Nagel, What is shaking in the sand box? Mater. Res. Soc. Bull. 19 (1994) 25.
[30] H.M. Jaeger, S.R. Nagel, R.P. Behringer, The physics of granular materials, Phys. Today 4 (1996) 32.
[31] H.M. Jaeger, S.R. Nagel, R.P. Behringer, Granular solids, liquids and gases, Rev. Mod. Phys. 68 (1996) 1259.
[32] H.M. Jaeger, S.R. Nagel, Dynamics of granular material, Am. Sci. 85 (1997) 540.
[33] Y. Du, H. Li, L.P. Kadanoff, Breakdown of hydrodynamics in a one-dimensional system of inelastic particles, Phys. Rev. Lett. 74 (1995) 1268.
[34] M.A. Meyers, Dynamic Behavior of Materials, Wiley, New York, 1994.
[35] N.N. Thadhani, Shock-induced chemical reactions and synthesis of materials, Prog. Mater. Sci. 37 (1993) 117–226.
[36] V.F. Nesterenko, M.A. Meyers, H.C. Chen, J.C. LaSalvia, Controlled high rate localized shear in porous reactive media, Appl. Phys. Lett. 65 (24) (1994) 3069–3071.
[37] K.S. Vecchio, M.A. Meyers, Shock synthesis in silicides-i. Experimentation and microstructural evolution, Acta Metall. Mater. 42 (3) (1994) 701–714.
[38] M.A. Meyers, L.H. Yu, K.S. Vecchio, Shock synthesis in silicides-ii. Thermodynamics and kinetics, Acta Metall. Mater. 42 (3) (1994) 715–729.
[39] I.P.H. Do, D. Benson, Micromechanical modeling of shock-induced chemical reactions in multi-material powder mixtures, Int. J. Plasticity 17 (2001) 641–668.
[40] P. Papadopoulos, On a class of higher-order pseudo-rigid bodies, Math. Mech. Solids 6 (2001) 631–640.
[41] J.M. Solberg, P. Papadopoulos, A simple finite element-based framework for the analysis of elastic pseudo-rigid bodies, Int. J. Numer. Meth. Eng. 45 (1999) 1297–1314.
[42] J.M. Solberg, P. Papadopoulos, Impact of an elastic pseudo-rigid body on a rigid foundation, Int. J. Eng. Sci. 38 (2000) 589–603.
[43] W.F. Ames, Numerical Methods for Partial Differential Equations, 2nd Edition, Academic Press, New York, 1977.
[44] O. Axelsson, Iterative Solution Methods, Cambridge University Press, Cambridge, MA, 1994.
[45] J.H. Holland, Adaptation in Natural and Artificial Systems. Ann Arbor Science, University of Michigan Press, Ann Arbor, MI, 1975.
[46] D.E. Goldberg, Genetic Algorithms in Search, Optim. Mach. Learning, Addison-Wesley, Reading, MA, 1989.
[47] L. Davis, Handbook of Genetic Algorithms, Thompson Computer Press, 1991.
[48] C. Onwubiko, Introduction to Engineering Design Optimization, Prentice-Hall, Englewood Cliffs, NJ, 2000.
[49] D.E. Goldberg, K. Deb, Special issue on genetic algorithms, Comput. Meth. Appl. Mech. Eng. 186 (2–4) (2000) 121–124.
[50] T.I. Zohdi, On the tailoring of microstructures for prescribed effective properties, Int. J. Fract., accepted for publication.